RZ 3664 (# 99674) 08/21/2006
Computer Science 4 pages

Research Report

In-Plane Coupling into Circular-Grating Resonators for All-Optical Switching

Asma Jebali, Rainer F. Mahrt

IBM Research GmbH
Zurich Research Laboratory
8803 Rüschlikon
Switzerland

Daniel Erni, Werner Bächtold

Communication Photonics Group, IFH
Swiss Federal Institute of Technology (ETH)
CH-8092, Zurich
Switzerland

Stephan Gulde

Institute of Quantum Electronics
Swiss Federal Institute of Technology (ETH)
CH-8092, Zurich
Switzerland

In-Plane Coupling into Circular-Grating Resonators for All-Optical Switching

Asma Jebali[1,2]*, Daniel Erni[1], Stephan Gulde[3], Rainer F. Mahrt[2], and Werner Bächtold[1]

[1] *Communication Photonics Group, IFH, ETH Zurich, CH-8092 Zurich, Switzerland*
[2] *IBM Zurich Research Laboratory, Säumerstrasse 4, CH-8803, Rüschlikon, Switzerland*
[3] *Institute of Quantum Electronics, ETH Zurich, CH-8093 Zurich, Switzerland*

** Tel: +41 44 632 31 28, Fax: +41 44 632 11 98, e-mail: jebali@photonics.ee.ethz.ch*

ABSTRACT
This paper addresses the issue of in-plane coupling into and out of circular-grating resonators with optical waveguides for all-optical switching applications. Two different designs are proposed: the first design consists in directly accessing the cavity with the waveguides. The second design is based on optimization with an evolutionary algorithm that randomly reshapes the gratings along the waveguides. Passive linear simulations for both approaches are performed with the finite-elements method, and the results will be presented.
Keywords: Circular gratings, in-plane coupling, all-optical switching.

1. INTRODUCTION

Circular-grating resonators (CGRs) are very attractive for potential applications in integrated optics such as lasing [1] and all-optical switching [2]. In this paper, we address the issue of in-plane coupling into and out of such resonators with optical waveguides for all-optical switching applications. In fact, once the coupling is optimized, a nonlinear Kerr material could be introduced into the microcavity to shift the resonance frequency and thus enable optical bistability [3]. In this paper, we restrict ourselves to passive linear simulations of the in-plane coupling into a circular-grating resonator.

For this purpose, the circular cavity has been designed accordingly as described in section 2. To achieve ultrafast all-optical switching, a trade-off between a high *Q*-factor and a high transmission, among other issues [2], is required. Therefore, in section 3, we propose a rather intuitive design based on direct access into the cavity with two optical waveguides, and in section 4, an alternative approach based on optimization with an evolutionary algorithm that randomly reshapes the gratings along the waveguides is presented. Extensive 2D numerical simulations using the finite elements method (FEM) are performed and the results are evaluated using the temporal coupled-mode theory (CMT) [4]. Section 5 summarizes this work.

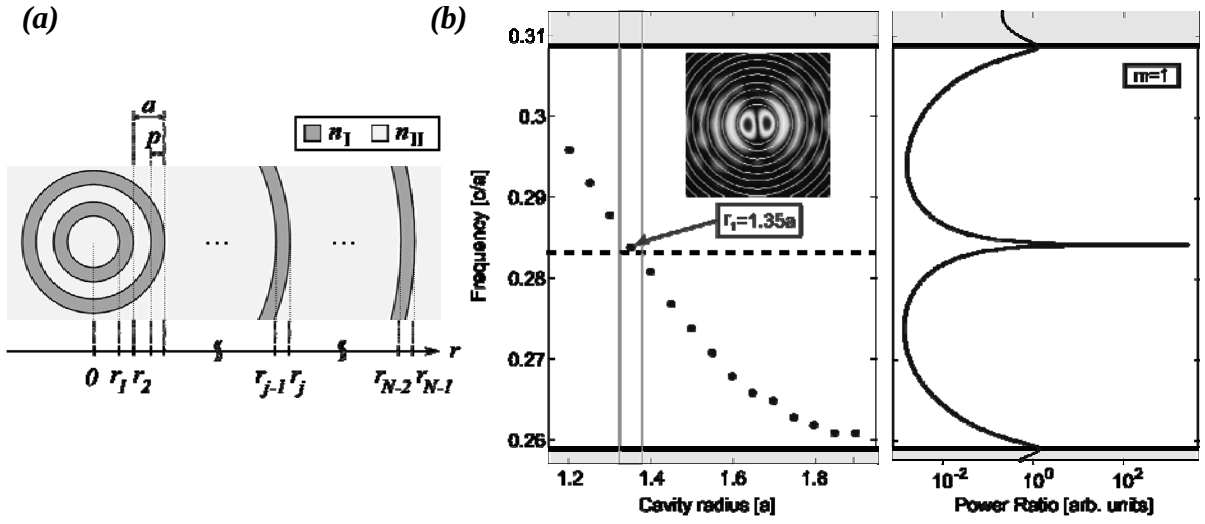

Figure 1. Cavity design: (a) Schematic representation of the structure geometry. (b) Scan over the cavity radii of the TMM resonances for the azimuthal order m = 1. The PBG is delimited by the shaded regions and its centre is indicated by a dashed line. The arrow points to the radius of interest r_1 = 1.35a, where the peak is in the centre of the PBG. The corresponding FEM calculation of the normalised electrical $|E_z|^2$-field distribution is shown as inset. The highlighted region (grey rectangle) selects the corresponding power-ratio plot [1,5].

This work has been supported by the Swiss National Centre of Competence in Research (NCCR) in Quantum Photonics (Project 9C).

2. CAVITY DESIGN

2.1 Free-standing cavity

To design the free-standing resonator without accessing waveguides, i.e. only the CGR, we need to determine all parameters specific to the geometry of the structure [Fig. 1(a)], namely the following: (i) The effective indices, $n_I = 1.6$ and $n_{II} = 1.96$. (ii) The lattice constant or grating period a to which the normalized frequency v [c/a] and the cavity radius r_1 [a] are normalized. (iii) The duty cycle $p/a = 0.45$. (iv) The mode order $m = 1$ (dipole mode) [5]. (v) The inner-cavity radius $r_1 = 1.35a$ is chosen so that its resonance lies in the centre of the photonic bandgap (PBG) to maximize the corresponding Q-factor. For this, we relied on the transfer matrix method (TMM) [1,5] and retrieved the resonance peaks lying in the centre of the PBG for a range of cavity radii, as shown in Fig. 1(b). (vi) The number of layers $N = 32$.

We apply our simulations in the visible/near-infrared range by choosing $\lambda = 870$ nm as operating wavelength. For the central normalized frequency $v_0 = 0.284$ c/a, where the dipole mode lies, we obtain a lattice constant of $a \sim 247$ nm and an inner-cavity radius of $r_1 = 1.35a \sim 333$ nm.

2.2 Coupled-mode theory (CMT)

To analyse the numerical simulations, we rely on the temporal CMT, which is based on a temporal differential equation describing the balance between incoming and outgoing field fluxes. This balance is expressed by [4]

$$\frac{1}{Q} = \frac{1}{Q_0} + \frac{2}{Q_e}, \tag{1}$$

where $Q = \omega_0\tau$ is the total quality factor of the device (ω_0 being the resonance frequency and $1/\tau$ the energy decay rate), Q_0 is the quality factor of the free-standing resonator, and Q_e the external quality factor associated with the access waveguides, as illustrated in Fig. 2(a). The power transmission of the device at resonance is then expressed by

$$T = \left| 1 - \frac{Q}{Q_0} \right|^2. \tag{2}$$

Therefore, accurate Q-factor calculations of the free-standing resonator are needed, but not easy to perform with the numerical tools available. Hence, we developed an analytical 2D model that calculates the Q-factor of the free-standing CGRs as well as their spectral response by means of TMM coefficients [6]. With the afore-mentioned parameters (section 2.1), the Q-factor of the free-standing CGR is then $Q_0 = 1892$.

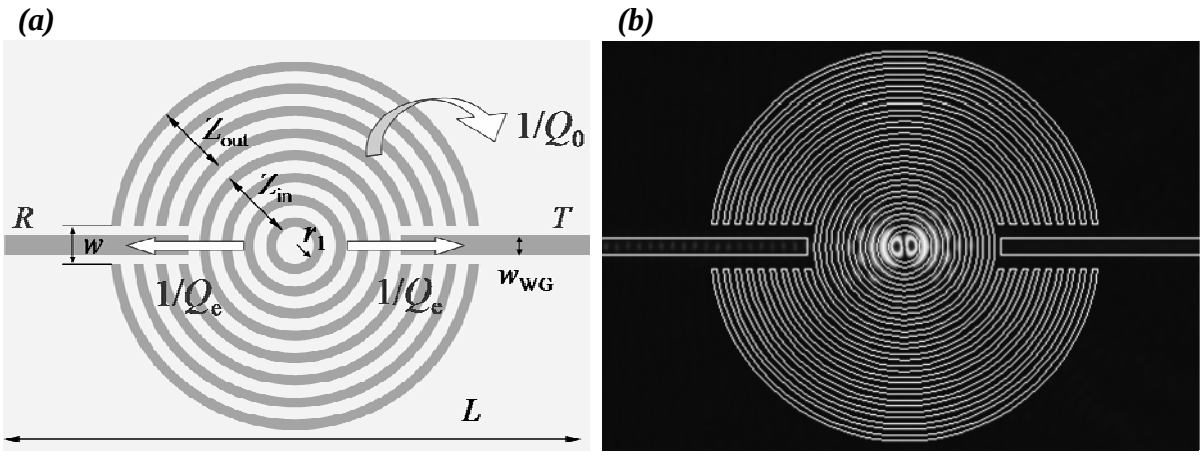

Figure 2. (a) Sketch of the circular-grating resonator coupled to two waveguides with the corresponding temporal coupled-mode theory parameters (R, T, Q_0, Q_e) and the geometrical parameters (r_1, Z_{in}, Z_{out}). (b) Corresponding 2D-FEM calculation of the normalised electrical $|E_z|^2$-field for the dipole mode (m = 1).

3. DIRECT ACCESS INTO THE CAVITY

In this section, we deal with the problem of efficient optical coupling between a CGR mode and a waveguide mode while keeping high Q-values. This coupling can be understood qualitatively as follows: if a resonator mode is excited, i.e. the resonator is filled with light; this light will eventually leak out of the resonator. For a device having negligible optical absorption and scattering losses, there are two ways for the light to leave the resonator: it either exits through the edges of the resonator uncollected or/and it is collected by the waveguide. One way to tackle the in-plane accessing problem is to let the waveguide partially penetrate into the high-Q_0 CGR. This ensures that the "leakage" of light out of the resonator mode is channelled into the waveguide. Any light in the grating resonator mode that is not directed into the waveguide mode encounters additional grating layers (i.e. rings) and is thereby reflected back into the resonator mode.

As illustrated in Fig. 2(a), in such geometry, the waveguides are designed to be monomode (width $w_{WG} = 1.5a$) and the openings, where they are embedded, have a width of $w = 4a$. The total device length is $L = 80a$. As a starting geometry, there are $Z_{in} = 7$ high-index rings between the two accessing waveguides and $Z_{out} = 9$ high-index rings outside. The sum of the layers is then $N = 2\cdot(Z_{in} + Z_{out}) = 32$. Figure 2(b) illustrates the corresponding 2D-FEM calculations of the normalised electrical $|E_z|^2$-field distribution for the dipole mode. It is clear that the dipole mode is nicely confined in the inner cavity.

After a first and rough design of the free-standing CGR with the TMM and spectral calculations with the FEM of the waveguide-accessed CGR, we proceed to a finer search to optimize the device performance. This is done by varying, for example, the number of 'inner' and 'outer' high-index layers (Z_{in} and Z_{out}). First, we increase the number of inner high-index layers ($Z_{in} = \{7,8,9\}$) and keep the outer ones constant ($Z_{out} = 9$). The resulting transmission spectra are analysed and the main CMT parameters are listed in Table 1. Moreover, Fig. 3(a) summarizes all these results in a T versus Q_0/Q graph corresponding to equation (2). The transmission $T \sim 55\%$ (mean value) does not vary a lot. However, the spectral linewidth obviously decreases by increasing Z_{in} and hence the total Q. This confirms that by increasing Z_{in}, we indeed increase the intrinsic Q_0, but by keeping Z_{out} constant, we do not improve the coupling and thus decrease Q_e, resulting in a constant transmission T.

Table 1. Varying the number of layers N via Z_{in} and Z_{out}.

(Z_{in}, Z_{out})	(9, 9)	(8, 9)	(7, 9)	(7, 12)	(7, 17)	(7, 9)*opt*
T [%]	53.06	57.08	54.94	53.16	**94.31**	61
λ [nm]	870.1	870.1	870.2	870.1	870.2	847
$\Delta\lambda$ [nm]	**0.66**	1.06	2.17	1.97	1.41	2.30
Q	**1315**	820	401	441	618	368
Q_0	4255	2837	1892	6383	**48560**	1892
Q/Q_0	0.309	0.289	0.212	0.069	0.013	0.195

Next, we keep $Z_{in} = 7$ constant and increase $Z_{out} = \{9,12,17\}$. The corresponding spectra show transmission ratios up to $T \sim 94\%$ for $(Z_{in}, Z_{out}) = (7,17)$. By increasing Z_{out} and keeping Z_{in} constant, we improve the intrinsic Q_0 and the external coupling Q_e. Thus, directly from equation (2), we increase the power transmission T and the total Q, which is, in this case, about 618. Higher Q-values can be achieved by larger gratings. To this point, no upper limit for Q has appeared in the 2D simulations. The corresponding results are depicted in Fig. 3(a) as triangles.

For an ultra-fast switching operation with a switching time switch $\tau_{switch} \sim Q\cdot\lambda_{res}/c = 1$ ps at $\lambda_{res} = 870$ nm yields $Q \sim 345$, the configuration $(r_1; Z_{in}, Z_{out}) = (1.35a;\ 7,\ 17)$ is hence best suited for a proper design, with a transmission $T > 94\%$ and an intrinsic $Q_0 > 48000$.

4. OPTIMISATION WITH EVOLUTIONARY SEARCH HEURISTICS

Another alternative to enhance the coupling into the inner cavity is to perturb the grating layers in the prolongation of the waveguide. This means one has to smoothen the abrupt transition between the waveguide and the CGR, i.e. better match the two modes. In fact, as often used in optical waveguiding, the tapering is the keyword for such a problem. There are so many possibilities to change the layers shape that a heuristic optimization method, which has the potential of finding the global optimum, is needed. The choice is the Breeder Genetic Algorithm (BGA), which is a special kind of steady-state evolutionary algorithm, as described in [5]. This class of heuristic optimization routines relies on the collective learning process within a population of individuals, each representing a possible solution to the optimization problem.

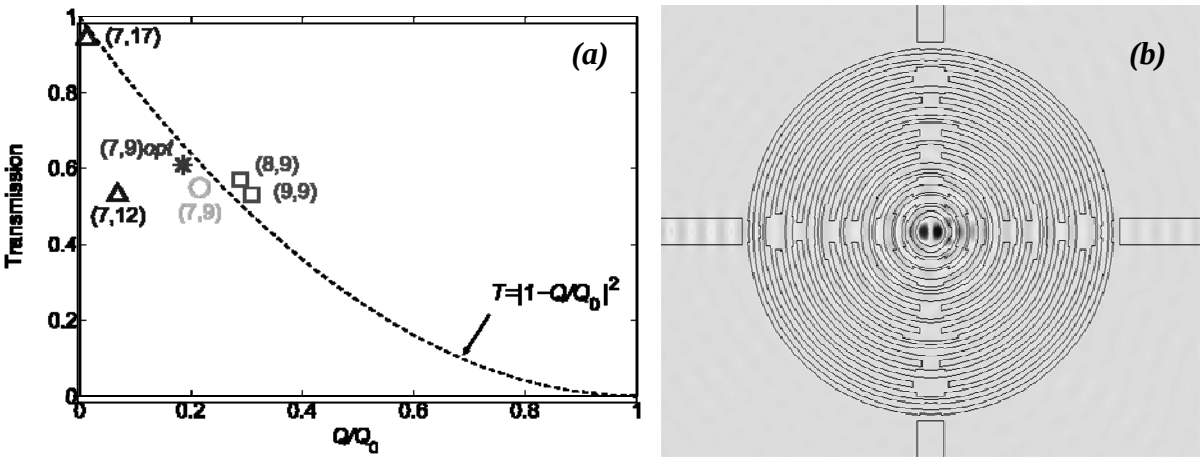

Figure 3: (a) Results of the analysis: T versus Q_0/Q, overview of all configurations investigated. The different (Z_{in},Z_{out}) pairs are shown. The circle represents the reference starting configuration (Z_{in},Z_{out}) = (7,9) with which all other configurations are compared. The star represents the same configuration optimized with the Breeder Genetic Algorithm, which 2D-FEM calculation of the electrical E_z-field is illustrated in (b).

The default configuration is the same as the one presented above. The fitness criteria for the algorithm are chosen to be a high transmission *T*, a high *Q*, as well as the enforced selection of the dipole mode. The cross-configuration and the dipole mode are chosen for an eventual all-optical switching application.

Some preliminary runs have been performed and one example of the results obtained is illustrated in Fig. 3(b), where a first configuration with corresponding electrical E_z-field distribution is shown. Note the cross configuration in this case, where two new waveguides were added perpendicularly in order to prevent any crosstalk for e.g. all-optical switching operation. The important resulting parameters are retrieved from the transmission spectra, are also listed in Table 1, and plotted in Fig. 3(a) as a star. The transmission *T* is about 61% and the *Q*-factor about 368. These preliminary results are very promising, but still subject to further improvements in additional optimization runs. Yet, for the same geometry parameters (r_1;Z_{in},Z_{out}) = (1.35*a*;7,9), the direct-access solution presented in section 3 (circle) and the optimized case (star) are equivalent. Therefore, one could use either approach for specific applications. This is also subject to further investigation.

5. CONCLUSIONS

The in-plane access of planar microcavities has been identified as a major issue and its systematic investigation is pioneered in this work. In fact, we focussed on the in-plane coupling into the CGRs via optical waveguides and proposed two approaches to deal with this issue, namely (i) a rather intuitive approach in which the waveguides directly penetrate into the CGR and (ii) an optimized one based on an evolutionary algorithm in which the grating layers are reshaped according to some fitness criteria (transmission, dipole mode, *Q*-factor). Both approaches were analyzed and exhibited different pros and cons for potential applications such as all-optical switching, lasing or electro-optical modulation. Nevertheless, in the scope of this paper, we did not investigate any such applications. Further work is to be done for nonlinear cavity materials and for 3D simulations.

ACKNOWLEDGEMENTS

We would like to thank Roman Kappeler as well as the other members of the Exploratory Photonics Group at IBM Zurich Lab for the fruitful discussions.

REFERENCES

[1] A. Jebali *et al.*: Lasing in organic circular grating structures, *J. Appl. Phys.* ***96****, 3043,* 2004.
[2] S. Gulde, A. Jebali, and N. Moll: Optimization of ultrafast all-optical resonator switching, *Opt. Exp.* ***13****, 9502,* 2005.
[3] R.W. Boyd: *Nonlinear Optics*, Academic Press, San Diego, CA, 2003.
[4] H.A. Haus: *Waves and Fields in Optoelectronics*, Prentice Hall, Englewood Cliffs, New Jersey, 1984.
[5] A. Jebali: *Optical Integrated Devices with Circular Grating Resonators,* PhD Thesis, *ETH Zurich Diss. No. 16530*, 2006.
[6] A. Jebali *et al.*: Analytical calculation of the *Q*-factor for circular-grating microcavities, *submitted,* 2006.